Dopant Concentration Profiles in Conducting Poly(*p*-phenylenevinylene) by Rutherford Backscattering Spectrometry

Michael A. Masse, Russell J. Composto, Richard A. L. Jones,* and Frank E. Karasz

Department of Polymer Science and Engineering, University of Massachusetts, Amherst, Massachusetts 01003

Received July 17, 1989; Revised Manuscript Received February 6, 1990

ABSTRACT: Elemental depth profiles have been obtained from AsF_5-doped poly(*p*-phenylenevinylene) films by using Rutherford backscattering spectrometry. Shallow arsenic penetrations were achieved with the AsF_5 source maintained at a temperature less than −53 °C. The arsenic penetration in a film doped for 10 days was approximately 1 μm. Further, the arsenic profiles are not characteristic of either Fickian or case II diffusion. A significant amount of oxygen is incorporated in these doped films. The RBS spectra indicated oxygen to be confined to the doped film surface layer (≈ 60 nm). This is consistent with the formation of surface arsenic oxide species. Nearly constant arsenic and fluorine concentrations are observed just below the film surface for relatively heavy dopings. These results suggest one AsF_6^- anion for every four to five PPV repeat units. When the measured dopant penetration is used, the lower limit to the intrinsic electrical conductivity of AsF_5-doped PPV is estimated to be 4×10^4 $(\Omega\ cm)^{-1}$.

Introduction

Doping processes in electrically conducting polymers are the route by which insulating polymers are converted to electrical conductors. These processes may be carried out chemically or electrochemically or by ion implantation.[1-3] In chemical doping typically a solid polymer film is contacted with a reactive liquid or vapor to create mobile charge carriers on the polymer chains. While many studies have investigated the relatively simple problem of diffusion of nonreacting small molecules in amorphous polymers,[4-7] far fewer studies have addressed the diffusion of dopant molecules into conducting polymers. With regard to diffusion several complexities are associated with the chemical doping process. First, conducting polymer matrices are usually semicrystalline. Thus, at least two pathways for diffusion exist in these materials. Second, the diffusant is reactive, forming new chemical species upon contact with the polymer, some of which may be side products and will subsequently counterdiffuse. Also, because of the reactivity of the dopants, especially AsF_5, side reactions not involved in conducting complex formation can occur. Dopant diffusion and the subsequently developed conducting polymer morphology will be of particular concern when considering the construction of electronic devices employing polymer layers as active components.[8-10]

Earlier studies of dopant diffusion in conducting polymers have employed weight gain measurements to evaluate the diffusion mechanism. Thus, Foot et al.[11] have demonstrated the AsF_5 doping of polyacetylene to be complicated by the simultaneous occurrence of diffusion, swelling, and reaction. This study found the arsenic uptake curve to be sigmoidal when plotted against $t^{1/2}$. From these results an induction period followed by Fickian diffusion is inferred. However, a full characterization of the diffusion behavior requires direct observation of concentration profile shapes as well as diffusant uptake measurements. Benoit et al.[12] used electron microprobe analysis to directly observe antimony profiles in microfibrillar SbF_5-doped polyacetylene films. This technique, however, only allowed examination at 5-μm spatial resolution and was only sensitive to the presence of antimony. In their study the diffusion profile was found to be characteristic of combined diffusion and chemical reaction and fixation.

Because of the unique chemistry involved in the synthesis of poly(*p*-phenylenevinylene) (PPV), it can be cast as dense, void-free films.[13] These films can be stretch-aligned, leading to a high degree of molecular orientation.[14] The films are highly crystalline, being composed of equiaxed (i.e., aspect ratio of 1.0) micellar crystallites with dimensions on the order of 5.0 nm.[15] Upon doping with a variety of chemical agents a crystalline conductive complex is formed.[16] The development of this conductive phase has been investigated using transmission electron microscopy.[15] The doping process in thin films (≈20 nm) is found to be characteristic of a nucleation and growth process with the doped phase nucleating at the grain boundaries at low doping levels and then subsequently growing at the expense of the insulating phase as the doping level is increased. Fully doped layers of 20-nm thickness were achieved after 4-h dopings with H_2SO_4. The question of how this doping process then proceeds through the thickness of bulk PPV films has yet to be addressed.

In this study we present Rutherford backscattering spectrometry (RBS) results for AsF_5-doped PPV. The purpose of this study has been to directly investigate the dopant diffusion profile and the chemical compositions of the electrically conducting films. RBS is especially useful in this application because of its high spatial resolution and its elemental sensitivity. The spatial resolution is at least 2 orders of magnitude greater than electron microprobe techniques, which have resolutions on the order of 1 μm. Also, all elements of atomic mass greater than the α-particle mass (i.e., $^4He^{2+}$) are simultaneously observable. Further, the experimental sensitivity of RBS to arsenic embedded in a hydrocarbon matrix is high. In fact, the atomic number contrast allows observation of much less than a single monolayer of arsenic on the PPV film surface. In this regard, AsF_5-doped PPV is an excellent material for RBS study.

* Present address: Department of Materials Science and Engineering and the Materials Science Center, Cornell University, Ithaca, NY 14853.

0024-9297/90/2223-3675$02.50/0

Scheme I

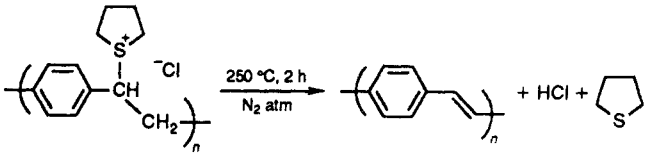

Experimental Section

Sample Preparation. The poly(*p*-xylylenetetrahydrothiophenium chloride) precursor polymer was synthesized as previously described.[17] The chemical structures of the precursor and PPV are shown in Scheme I. Films of the precursor polymer were cast from aqueous solution. The films were highly uniaxially oriented to an elongation of 1000%. Details of the processing have been discussed elsewhere.[18] The conversion to fully conjugated PPV was performed by annealing the oriented films under nitrogen at 250 °C for 2 h. Elemental analysis of the annealed films, performed by the University of Massachusetts Microanalytical Laboratory, indicated a composition of 92.0 wt % carbon and 5.7 wt % hydrogen (theoretical; 94.1% C, 5.9% H). The amounts of sulfur, oxygen, and chlorine were less than 0.3%, indicating nearly complete conversion from precursor to PPV. The resulting films were 2 μm in thickness.

Doping. Arsenic pentafluoride was used to chemically oxidize or "dope" PPV films. The following electron-transfer fluorine-disproportionation reaction is responsible for increases in conductivity.

$$2\mathrm{PPV(s)} + 3\mathrm{AsF_5(g)} \rightarrow 2[\mathrm{PPV^+AsF_6^-}](\mathrm{s}) + \mathrm{AsF_3(l)} \quad (1)$$

The AsF_6^- anion has been previously observed in AsF_5-doped PPV,[19,20] confirming the occurrence of the above reaction. The AsF_5 was obtained from the Ozark-Mahoning Co. and was purified by three freeze–pump–thaw cycles prior to use. The dopant was stored in a glass bulb equipped with a cold finger. The cold finger was maintained at a constant temperature (±0.5 °C) over the course of a single doping reaction. In this way the vapor pressure of the dopant could be controlled by employing vapor–liquid equilibrium of the AsF_5. Further, this arrangement could also be used to cold-trap the less volatile side product by operating below the melting point of AsF_3 (−6 °C). For this study the cold finger was held at −70.5 °C, giving a measured AsF_5 vapor pressure of 280 mmHg. The PPV films were contained in glass vessels, which were evacuated to 10^{-4} mmHg before doping. PPV films were attached to silicon wafer sections by using a thin layer of epoxy adhesive. Care was taken to avoid the complications of AsF_5 reaction with epoxy using minimal amounts and by exposing no epoxy surface. PPV samples prepared in this fashion were exposed to dopant vapor only at the air interface. Further, because the polymer chains were aligned parallel to the silicon substrate, diffusion proceeded mainly in a direction perpendicular to the chain axis. Doping was performed by backfilling the evacuated vessel with AsF_5 vapor, and the doping or contact time was controlled. The samples were vacuum pumped for 24–36 h after doping to remove residual side products. The samples were then sealed in evacuated glass ampules.

Conductivity Measurements. The bulk electrical conductivity of selected films was measured as the films were doped by using a four-terminal geometry. Four platinum wires were attached transversely across the film widths by using a carbon black-graphite adhesive (Acheson electrodag 502). The electrical resistance, R, of the films was determined by passing a known current through the outer two leads and measuring the voltage between the inner two leads. This geometry minimizes the effect of contact resistance. Further details of resistance measurements on conducting polymer films have been previously published.[21] The conductivity was then calculated according to

$$\sigma = (1/R)(L/A) \quad (2)$$

where L is the length between the voltage measuring leads and A is the bulk cross-sectional area. It is important to note that eq 2 calculates the conductivity under the assumption that the sample is homogeneously doped through its entire cross-sectional area. As the RBS results will show, this assumption is not always valid.

Rutherford Backscattering Spectrometry. The utility of Rutherford backscattering spectrometry (RBS) as an analytical tool derives from its sensitivity to sample nuclei mass and nuclei depth. Furthermore, samples do not require handling and sectioning as do samples for microprobe analysis. In RBS a monoenergetic beam of α-particles ($^4He^{2+}$) impinges on a sample. Some fraction of the α-particles are backscattered by elastic collisions with target nuclei. The energy and yield of these backscattered particles are then detected. The energy, E, of a backscattered particle is given by

$$E = KE_0 \quad (3)$$

where K is the kinematic factor and E_0 is the incident energy of the α-particle. The kinematic factor depends upon the masses of the two particles involved in the collision. In general, the kinematic factor is expressed as

$$K = \{[1 - (m/M)^2 \sin^2\Theta]^2 + (m/M)\cos\Theta\}^2/[1 + (m/M)]^2 \quad (4)$$

where Θ is the scattering angle, M is the sample nuclear mass, and m is the incident particle mass (i.e., $m = 4$ for ^4He). Given an incident α-particle energy of 2.14 MeV, the backscattered energies from C, O, F and As nuclei on the sample surface will be 538, 773, 913, and 1730 keV, respectively. These energies will be hereafter referred to as surface energies for these specific elements.

Equation 3 will only apply if no energy loss mechanisms are operative (i.e., backscattering from the film surface). In the case of α-particles backscattered from below the film surface, the particle loses energy due to Coulombic interactions with electrons and small-angle scattering by sample nuclei. Thus, the energy of an α-particle scattered from a depth x is

$$E = KE_0 - [\mathrm{S}]_x \quad (5)$$

where [S], the energy loss factor, describes the energy lost on the inward and outward paths. Thus, the energy spectrum will allow elemental depth profiling. Assuming constant but different energy losses for the inward and outward paths of a scattered particle, the energy loss factor is expressed as

$$[\mathrm{S}] = \{(K/\cos\Theta_1)(\mathrm{d}E/\mathrm{d}x)|_{\mathrm{in}} + (1/\cos\Theta_2)(\mathrm{d}E/\mathrm{d}x)|_{\mathrm{out}}\} \quad (6)$$

where K is the kinematic factor for the nucleus scattering the particle of interest, Θ_1 is the angle between the incident particle path and the sample surface normal, Θ_2 is the angle at which the particle is scattered, and x is the spatial variable representing distance below the sample surface. When eq 6, a mass density of 1.22 g/cm^3, and tabulated elemental stopping cross-sections[21] of carbon and hydrogen are used, the energy loss factor for pristine PPV (C_8H_6) is calculated as 313 eV/nm for particles backscattered from carbon nuclei.

The composition, or number of atoms of each type, in a sample is determined from the total number of detected particles or yield. The yield from a thin layer (t) of atoms at the sample surface is

$$Y = b(\Theta)\,\Omega Q(Nt) \quad (7)$$

where Q is the number of incident particles, Ω is the solid angle subtended by the detector, Nt is the number of nuclei per square centimeter in the layer, and $b(\Theta)$ is the differential scattering cross section given by

$$b(\Theta) = K(Z_1Z_2e^2/4E)^2 \sin^{-4}(\Theta/2) \quad (8)$$

where Z_1 and Z_2 are the atomic numbers of the target nucleus and the α-particle, E is the particle energy immediately before scattering, and K is the kinematic factor. Because of the factor Z_1^2, RBS is quite sensitive to elements of large atomic number.

The ratio of the surface yield for a target atom and a reference carbon atom is

$$H/H_C = (b/b_C)(N/N_C) \quad (9)$$

where N is the atomic density of the target nuclei. Thus, a measurement of the surface yields combined with the known cross sections allows one to determine the number of dopant atoms per carbon.

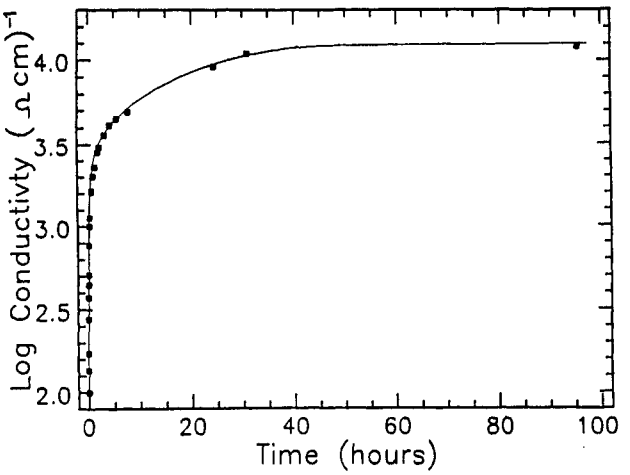

Figure 1. Time response of bulk conductivity for an AsF_5-doped film. The dopant vapor pressure was 280 mmHg, and the film thickness was 2 μm. All film surfaces were exposed during doping.

In this study we report normalized yield values given as

$$Y_N = Y/[\Omega Q(1/\cos\theta_1)] \quad (10)$$

which are only material dependent. As can be seen from eq 7, the number of atoms of species i in a given layer is proportional to its measured yield. Therefore, the total number of atoms of i in a sample is proportional to the yield integrated over energy.

For a more thorough discussion of backscattering physics the reader is referred to the literature.[21] The calculations were performed by using the RUMP simulation program developed by L. R. Doolittle.[22]

Rutherford backscattering spectrometry was performed at the Ion Beam Facility of the Materials Science and Engineering Department, Cornell University (Ithaca, NY). An α-particle beam was accelerated to 2.14 MeV by using a tandem electrostatic accelerator (General Ionex). The samples were mounted on the holder under a nitrogen atmosphere and were transferred to the instrument by using a valved load-lock. Backscattered particles were detected at an angle of 173°. The beam current was approximately 15 nA. Spectra were collected at room temperature for an integrated charge of 5 μC over an approximate spot size of 1 mm^2. Because the spot size is much larger than the PPV crystallite size (i.e., 5.0 nm), the results thus obtained represent the average diffusion character over a statistical collection of crystallites and disordered grain boundaries. The multichannel analyzer channel width was approximately 18 keV. Thus, an estimated spatial resolution of 60 nm exists in samples having energy loss factors of 300 eV/nm (i.e., pristine PPV).

The occurrence of beam damage in doped films was assessed by sequentially collecting spectra at 0.5-μC intervals from a single spot. Both the carbon and arsenic normalized yields were constant with increasing charge up to 15 μC, indicating beam stability of these elements. In lightly doped samples the oxygen and fluorine yields showed signs of beam-induced degradation up to 5 μC, after which the yields became stable. This partial degradation occurred at both room temperature and at liquid-nitrogen temperatures (−196 °C). While the O and F species showed beam-induced degradation, the C/As ratio and As profile shapes will be unchanged. The surfaces of the films were also inspected for α-particle-induced ablation by using scanning electron microscopy. While some cracking was apparent, no serious ablation was observed. The RBS spectra were found to be reproducible within a single sample. Spectra obtained from several spots along the length of a sample showed only a few percent variation in the yields for all elements.

Results

Electrical Conductivity. In the undoped or pristine state PPV has an electrical conductivity of $<10^{-10}$ $(\Omega\ cm)^{-1}$. Figure 1 shows the electrical conductivity as a function of AsF_5 doping time for a dopant vapor pressure of 280 mmHg. In the initial hour of doping the conductivity increases to 10^3 $(\Omega\ cm)^{-1}$. After this initial period the conductivity increases more slowly, reaching a limiting conductivity of 1.25×10^4 $(\Omega\ cm)^{-1}$. The appearance of the film changes from being translucent and yellow in the insulating state to having a highly reflective surface and a metallic golden luster in the fully doped film.

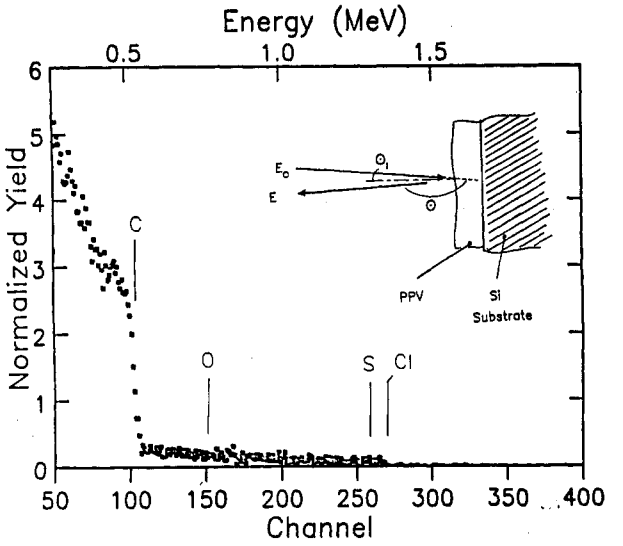

Figure 2. RBS spectrum of pristine PPV. The surface energies of C, O, S, and Cl are indicated. The inset schematically shows the sample configuration and experiment geometry.

The immediate increase in conductivity indicates the rapid formation of a continuous conductive pathway along the length of the film. Further, the weight uptake of dopant by the films can be measured simultaneous to conductivity measurements. For one sample doped to 2.5×10^1 $(\Omega\ cm)^{-1}$ a weight gain of less than 1% of the pristine mass was measured.[23] Samples highly doped with AsF_5 typically have weight gains on the order of 150% of the pristine mass.[16] Thus, the early observation of high conductivity occurs with a relatively small percentage of the PPV being converted to the conductive complex. RBS results concerning the physical and chemical changes associated with the increased conductivity are now presented.

Rutherford Backscattering Spectrometry. The backscattering spectrum for pristine PPV (C_8H_6) is shown in Figure 2. As expected carbon is the nucleus primarily observed. The slight background near 1.3 MeV may arise from residual S and Cl from the precursor polymer. Although bulk elemental analysis for S and Cl indicated trace amounts at most, the sensitivity of RBS allows observation at the impurity level. No O is observed in the pristine films.

After doping As and F nuclei are observed in addition to C. Figure 3 shows the RBS spectrum for a PPV sample exposed to AsF_5 vapor for 5 days. Here, a significant O peak is also observed even though samples were evacuated to 10^{-4} mmHg before doping and all handling was done in an inert atmosphere. The backscattered particles for all nuclei are observed at their surface energies, indicating the presence of C, O, F, and As at or near the doped film surface. Further, for this particular doping condition the full-widths at half-maximum of As and F peaks are greater than the instrumental resolution and show low-energy tails. Thus, penetration of As and F has occurred. The O peak is narrow and within the instrumental resolution, suggesting confinement to the film surface.

Figure 4 shows only the As region of the RBS spectra for PPV films exposed to AsF_5 vapor for 1 h, 4 h, 5 days,

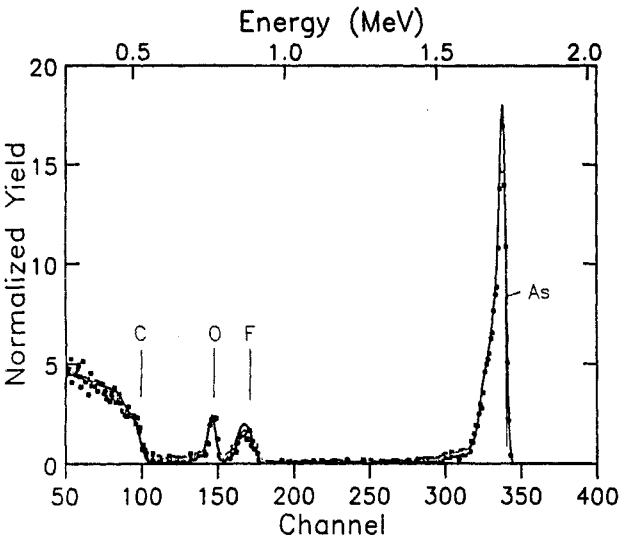

Figure 3. RBS spectrum of AsF_5-doped PPV (280 mmHg, 5 days). The surface energies for C, O, F, and As are indicated. The solid line represents the RUMP simulation (see text).

and 10 days. At 1 h the As nuclei are confined within the first 60 nm of the film. After a 4-h doping the yield of the As peak has increased, but the peak displays only a slightly asymmetric tail on the low-energy side. This increase in yield indicates that more As has been incorporated into the near surface layer but has not penetrated into the surface beyond the instrumental resolution. As doping is continued to 5 and 10 days the surface amounts of As increase again and dopant penetration is apparent. There is a high surface concentration of As at these long doping times. In fact, the surface concentration is higher for the 5-day doping. This is attributed to a high concentration of arsenic oxides at the film surface as will be discussed later. It is important to note that the As peak profile does not fall off smoothly on the low-energy side. At depths below the surface the yields decrease to a nearly constant region and only then fall off smoothly to zero yields. The As penetration depth is given approximately by the scale included in Figure 4. This depth scale is calculated by using the energy loss factor for pristine PPV. A more precise determination of the As penetration requires consideration of As, F, and O incorporation. This will be discussed in reference to the RUMP simulations. Regardless of the absolute depth scale, it is clear that the As penetration depths for these doping conditions are shallow with respect to the total film thickness.

The carbon–oxygen–fluorine region of the RBS spectrum is shown in Figure 5 for pristine PPV and for PPV doped for 4 h and 5 days. As doping proceeds both F and O yields increase. While the F and O yields represent the minimum concentrations because of beam-induced degradation, the profile shapes are assumed to be unchanged. At 5 days the F peak exhibits a significant breadth while the O peak is relatively narrow. Thus, there is preferential penetration of F, with O being mainly confined to the doped film surface layer. The carbon edge appears at its surface energy at all doping levels. The carbon profile shape, however, does suffer a subtle change. The yield at the surface is slightly lessened. As will be apparent from the simulations the decreased carbon yield is entirely due to a dilution effect; the number of C nuclei per unit volume has been reduced at the surface by incorporation of As, F, and O nuclei.

RUMP Simulations and Depth Profiles. Computer simulations of the RBS spectra were performed by dividing the film thickness into many layers and requiring each layer

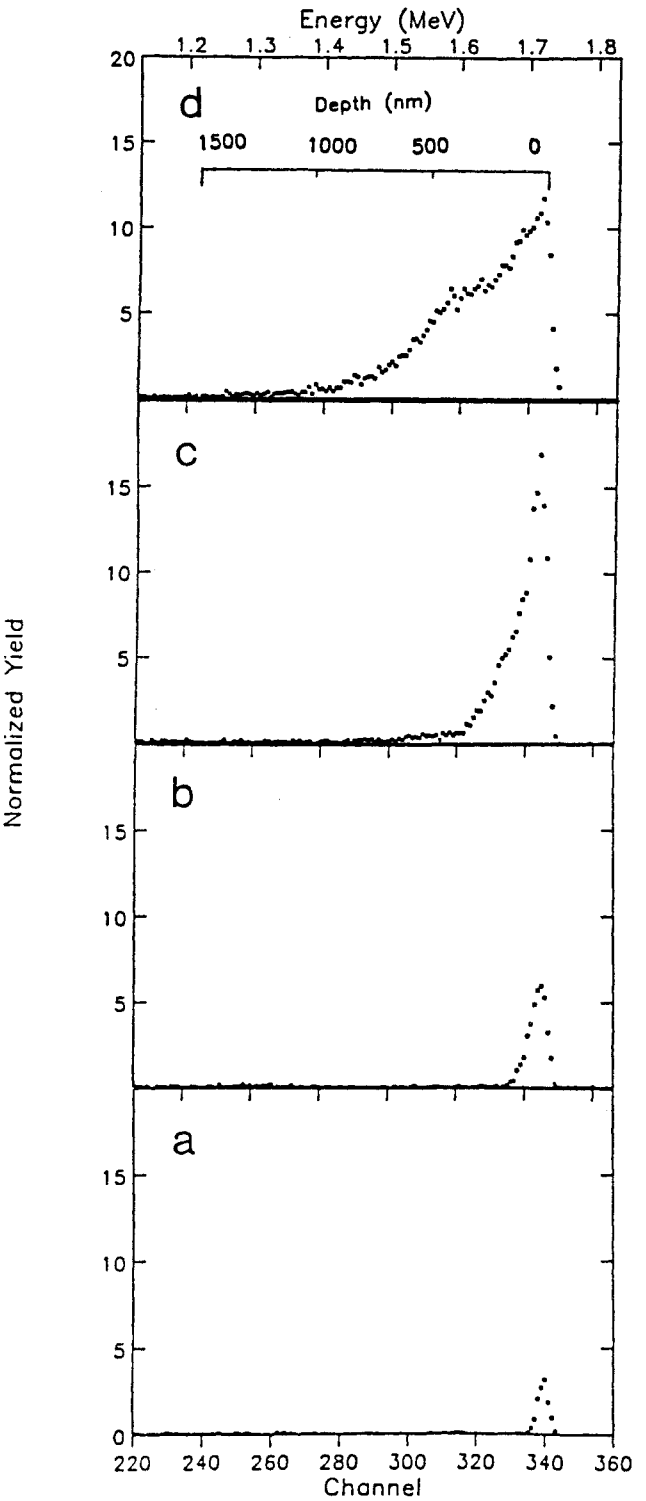

Figure 4. Arsenic region of the RBS spectra for various doping times: (a) 1 h, (b) 4 h, (c) 5 days, (d) 10 days. An estimated depth scale for the As nuclei is indicated (see text).

to be chemically homogeneous. Because of the limited number of layers available in the RUMP program (i.e., 25), a constant layer thickness could not be used to simultaneously fit profile depth and intensity. Thus, greater thicknesses were used for the deeper layers where the change in profile shape was more gradual. The same depth protocol was used for all simulations. The composition of each layer was referenced to the polymer repeat unit. Thus, each layer had the stoichiometry $C_8H_6As_xF_yO_z$ where x, y, and z were variable. The simulated spectrum was then fit to the data by iteratively modifying the composition of each layer. Typically, the

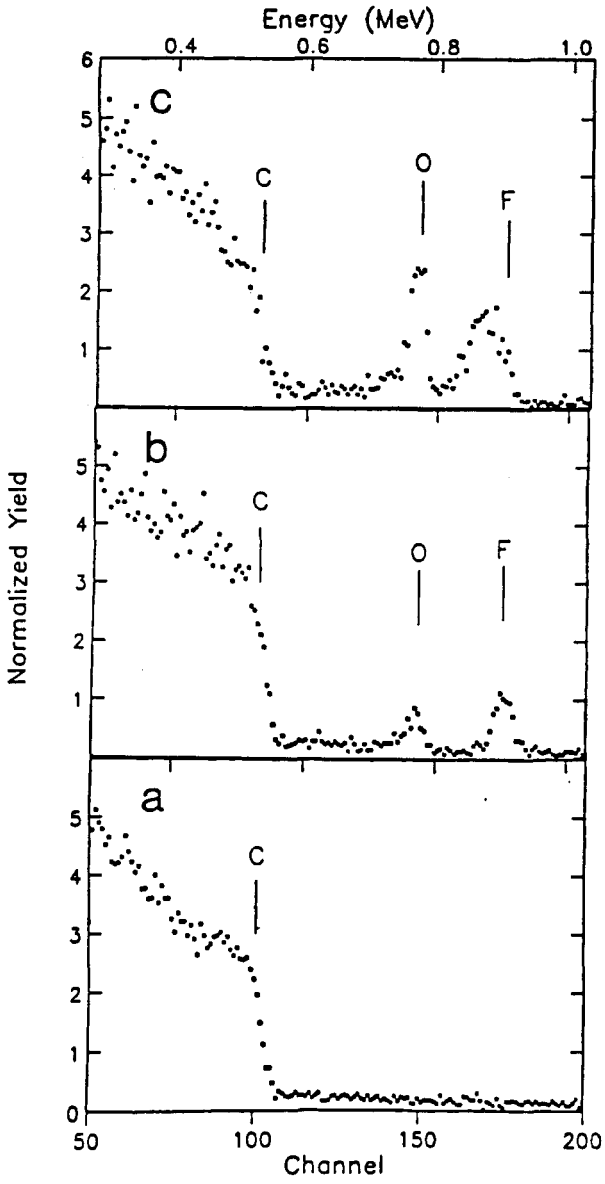

Figure 5. Carbon, oxygen, and fluorine region of the RBS spectrum for various doping times: (a) pristine PPV, (b) 4 h, (c) 5 days. The surface energies of C, O, and F are indicated.

depth scales in RBS are given in areal atomic densities (i.e., atoms per cubic centimeter). The calculated atomic density for pristine PPV is 1.008×10^{23} atoms/cm^3. This value has been used in the conversion from areal atomic density to depth. The simulated spectrum for the 5-day doped film is shown by the solid line in Figure 3. The entire spectrum is well fit using this approach. The layer thicknesses and compositions for the simulated 5-day doping spectrum are shown in Table I. Here the depth is the distance below the surface at which the layer begins and is given in nanometers.

When the simulated models were used as a reference to calculate the variation in atomic density with layer composition, the atomic depth profiles were calculated from the RBS spectra. Figure 6 shows the As penetration for 4-h, 5-day, and 10-day dopings. At 4 h the As profile decreases smoothly from ≈0.25 As atoms per PPV repeat to zero at 100 nm. For the 5-day doping the surface concentration of As is near 0.9. This falls steeply to a knee in the profile at 120 nm. The concentration at the knee is ≈0.15. At greater depths the As concentration decreases smoothly, reaching the noise level at 250 nm. The profile for the 10-day doped sample is qualitatively similar to the 5-day profile. The surface concentration is 0.6 and falls to a nearly constant value of 0.22 between depths of 120–300 nm. Beyond this depth the concentration drops smoothly to zero at approximately 800 nm (not shown).

Table I
Simulated Composition of AsF_5-Doped PPV (280 mmHg, 5 days)[a]

depth, nm	arsenic, x	fluorine, y	oxygen, z
0.0	9.000	3.00	15.00
20.0	7.000	3.00	13.00
40.0	3.000	3.00	10.00
70.0	1.250	3.00	3.00
100.0	0.900	3.00	1.50
130.0	0.700	3.00	1.00
160.0	0.550	3.00	0.80
190.0	0.450	2.00	0.70
220.0	0.350	1.30	0.60
270.0	0.150	0.80	0.50
320.0	0.100	0.60	0.00
370.0	0.070	0.50	0.00
420.0	0.050	0.40	0.00
470.0	0.045	0.04	0.00
520.0	0.040	0.30	0.00
570.0	0.035	0.25	0.00
620.0	0.030	0.20	0.00
670.0	0.025	0.15	0.00
720.0	0.020	0.10	0.00
1000.0	0.000	0.00	0.00

[a] Each layer is chemically homogeneous with a stoichiometry of $C_8H_6As_xF_yO_z$.

Discussion

The As profiles at 5- and 10-day doping are not characteristic of Fickian diffusion and imply a more complex diffusion mechanism. If the diffusion were Fickian, then the As concentration would decrease smoothly from its surface concentration, C_o, according to the following error function profile as the distances from the surface, x, increased.[24]

$$C = C_o \operatorname{erfc}(x/2\sqrt{Dt}) \tag{11}$$

Here, D is the effective diffusion coefficient and t is the doping time. In Figure 6 the experimental data are compared to calculated Fickian concentration profiles. The profiles were calculated by using eq 11 with $D = 5.5 \times 10^{-10}$ cm^2/s. Clearly, Fickian diffusion is not obeyed in this system. Another possibility is case II diffusion commonly seen in rubbery, amorphous polymers.[24] In this situation a front of constant concentration, C_o', would exist near the surface and this would be preceded by a Fickian precursor front. The As profiles observed in this system do not show a surface layer of finite thickness having a constant concentration. While some region of nearly constant concentration exists 200–300 nm below the surface, a strong surface gradient is also evident in these doped films, indicating a more complex diffusion mechanism.

In addition to the qualitative evaluation of diffusant profile shape the diffusion character can be evaluated by comparing the change in the integrated amount of diffusant with time. For Fickian diffusion[24] the diffusant uptake increases as $t^{1/2}$ while case II[7] uptake increases as t. As discussed in the Experimental Section the total amount of As incorporated into the doped films is proportional to the integrated peak areas. The As peak area is plotted against doping time in Figure 7. After the initial doping period (1–4 h) the As incorporation is linear with time to 10 days. Note that a simple As uptake measurement would indicate case II diffusion. However, the profile shape has been directly observed, and case II behavior is discounted on this basis.

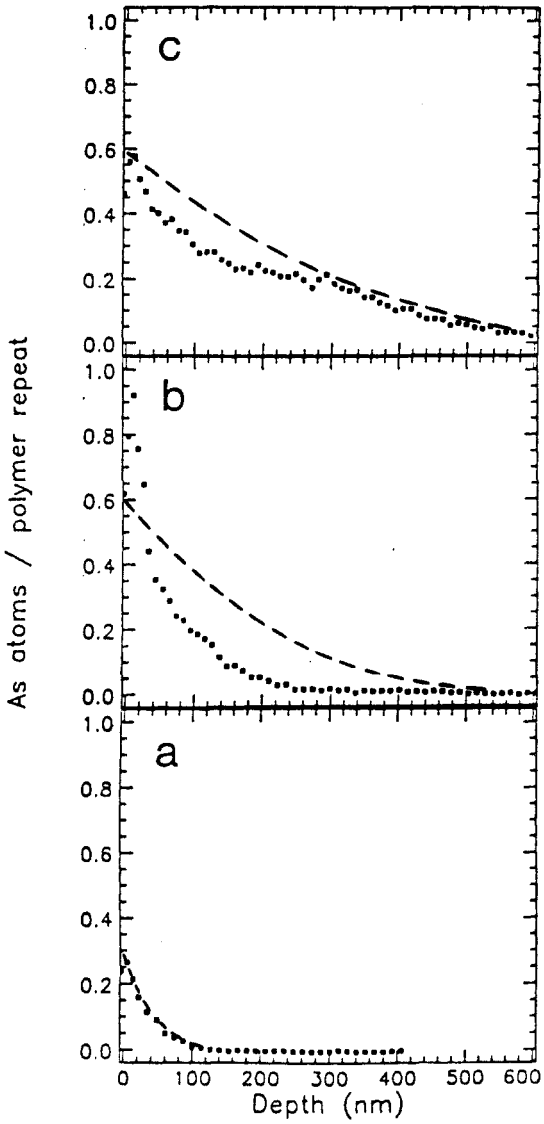

Figure 6. Depth profile of As in films doped for various times: (a) 4 h, (b) 5 days, (c) 10 days. The points represent the experimental data. The dashed line is the Fickian concentration profile calculated with $D = 5.5 \times 10^{-10}$ cm^2/s.

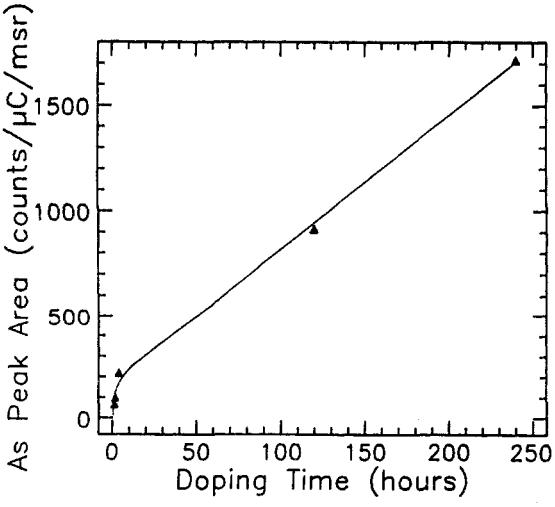

Figure 7. Integrated areas for the As peak as a function of doping time.

When the elemental information gained from RBS is used, an analysis of the sample stoichiometry can be performed. For the AsF_5–PPV system some chemical binding information has been previously determined. Wide-angle X-ray diffraction of AsF_5-doped PPV has suggested the presence of As_2O_5 and hydrates of this oxide to be formed during doping.[20] Presumably, these compounds are formed through reaction of AsF_5 with residual O_2 or H_2O even though high-vacuum and inert-gas environments have been employed. Further, the presence of the AsF_6^- anion in AsF_5-doped PPV has been confirmed by using FTIR and XPS.[20] Also, mass spectrometry of the thermolysis products of doped films has not revealed fluorinated hydrocarbons, suggesting an absence of fluorinating side reactions in the AsF_5-doping process. One simple chemical model can thus be assumed: $(C_8H_6)_m[(C_8H_6^{\delta+})_x(AsF_6^-)]_n(As_2O_5)_p$. This model, however, cannot be satisfactorily fit by using the RBS data. For instance, with the 5-day doped sample the elemental surface composition is $C_8H_6As_9F_3O_{15}$ (see Figure 6). If all the F and O are assumed to be incorporated in the films as AsF_6^- and As_2O_5, respectively, then an excess of 2.5 As atoms remains. Further, allowing the presence of arsenic oxide hydrates worsens the fit. The difficulty in evaluating the doped film stoichiometry is partly attributable to beam-induced degradation of F and O.

While the exact chemical composition of the doped films is uncertain the elemental profiles of O and F show that the arsenic oxides are confined to the film surface and the arsenic fluoride diffuses into the film. Further, Figure 8 shows the F/As atomic ratio as a function of depth for different doping conditions. This ratio is calculated from the simulated spectra. For all of the doping times shown the F/As ratio is less than 2 at the surface. At increasing depths this ratio tends toward 6, the expected ratio for AsF_6^-, even though beam-induced degradation of F occurs. The presence of other arsenic fluoride species (i.e., AsF_5 and AsF_3) would serve to lower the observed F/As. As expected, AsF_6^- is suggested as the dopant anion by the F/As ratio. Binding of As in the form of oxides is expected to be primarily responsible for the low F/As ratios at the film surface.

X-ray diffraction results indicate that only one structure exists for the AsF_5–PPV complex.[16] Therefore, one dopant to polymer ratio must exist which is characteristic of the conducting complex. The dopant to polymer repeat ratio can be evaluated from the stable As profiles. As can be seen from the 10-day doping profile (Figure 6c), a region of nearly constant As concentration exists with 0.25–0.20 As atoms per polymer repeat. Thus, one AsF_6^- anion for every four to five polymer repeat units is suggested. This is consistent with results obtained from PPV electrochemically oxidized by using AsF_6^- as the counterion. The electrochemical behavior is reversible up to an oxidation level of 25 mol % (i.e., four PPV repeats per AsF_6^- counterion).[25] A similar stoichiometry is also suggested from F/C ratios obtained from X-ray photoelectron spectroscopy of lightly doped PPV surfaces.[20] This is somewhat lower than the result suggested by X-ray diffraction from the conducting phase (i.e., one AsF_6^- for every two PPV repeat units).[23] This may be due to incomplete doping in the grain boundary regions of the semicrystalline conducting films.

A physical model of AsF_5-doped PPV is schematically presented in Figure 9. This model is intended to represent only the qualitative features of the dopant concentration profiles for samples that have been subjected to heavy dopings. In the model an arsenic oxide surface layer exists. Below the surface layer resides a layer of nearly constant dopant concentration ($C_8H_6^{\delta+}/AsF_6^- = 4$–5), and at greater depths the dopant anion penetrates the undoped polymer as a precursor front. This profile bears some similarity

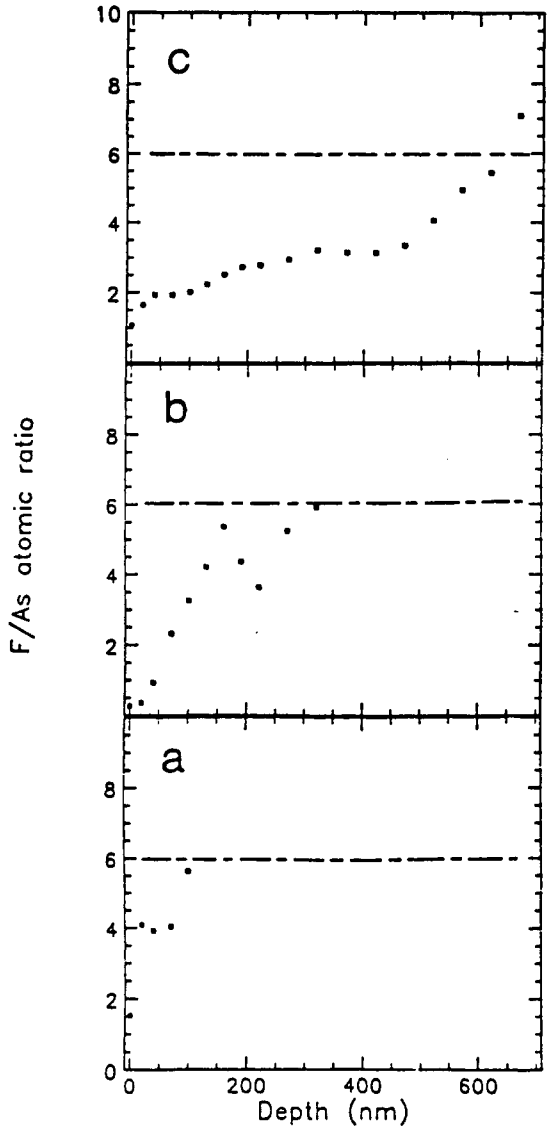

Figure 8. Fluorine to arsenic atomic ratio as a function of depth for various doping times: (a) 4 h, (b) 5 days, (c) 10 days.

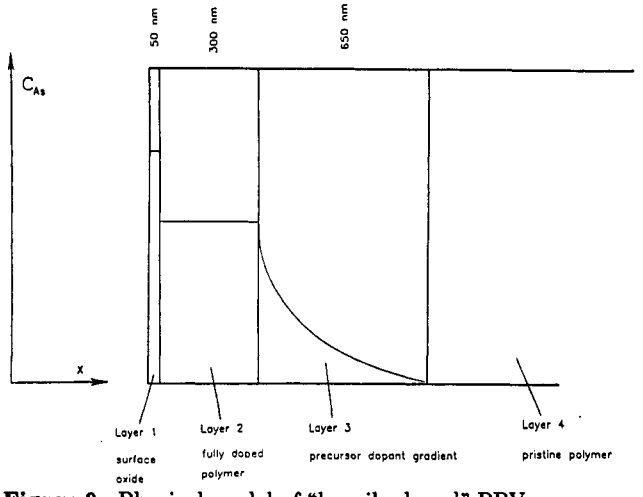

Figure 9. Physical model of "heavily doped" PPV.

to case II diffusion fronts observed in the diffusion of small molecules in glassy polymers.[7] The polymer doping process, however, is compounded by the simultaneous diffusion and reaction of AsF_5 and therefore cannot be simply classified as either Fickian or case II diffusion.

It is important to realize that these results apply to specific doping conditions. Preliminary experiments in our laboratory have shown that dopant penetrations of 1 μm can be achieved in PPV after only a 1-h exposure to an AsF_5/AsF_3 vapor mixture. Further, the profile shapes appear even more similar to those seen in case II diffusion. The deeper dopant penetrations at these conditions are attributed to the plasticizing effect of AsF_3 in AsF_5-doped polymers. This effect has been previously noted in AsF_5-doped polyacetylene[11] and poly(*p*-phenylene sulfide).[26]

Table II
PPV Film Conductivity Normalized to Doped Layer Thickness, *d*

doping time	resistance (Ω)	$\sigma^{bulk} \times 10^4$, $(\Omega\ cm)^{-1}$	$d \times 10^7$, cm	$\sigma^{norm} \times 10^4$, $(\Omega\ cm)^{-1}$
1.0 h	2.23	0.206	60.0	3.5
2.0 h	1.58	0.291	60.0	4.9
4.0 h	1.13	0.407	100.0	4.1
5.0 days[a]	0.368	1.250	250.0	5.0

$(L/A)^{bulk} = 4660\ cm^{-1}$
$(L/A)^{norm\ b} = (0.932)(1/2d)\ cm^{-1}$
see eq 2

[a] This sample was doped for only 4 days. The σ^{norm} calculation was done by using the penetration depth for the 5-day sample. Thus, σ^{norm} for this sample represents a lower limit to the intrinsic conductivity at 5-day doping. [b] Twice the dopant penetration is used to calculate the conductivity since both sides of these films were exposed to AsF_5.

As previously stated, the conductivity of bulk films doped in the manner employed here is calculated by using the entire film thickness. Clearly, such calculations are not representative of the true material properties since the doping is strongly heterogeneous forming shallow doped layers. In this case, it is clear that the charge carriers created by doping will only reside in a relatively shallow conducting layer. Thus, a better calculation is one that takes into account the actual doped layer thickness. Table II shows the conductivities calculated by using the entire film thickness, σ^{bulk}, and the measured doped layer thickness, σ^{norm}. For the purpose of these calculations the doped layer thickness has been taken as the maximum observable As penetration depth. With this calculation an intrinsic conductivity representative of the actual ability of PPV chains to support charge carrier transport is estimated. The normalized conductivity, σ^{norm}, is calculated as $3.5 \times 10^4\ (\Omega\ cm)^{-1}$ for a 1-h doping and $5.0 \times 10^4\ (\Omega\ cm)^{-1}$ for a 5-day doping. Thus, the normalized conductivities are considerably higher than the bulk values. These values, while higher than previously reported PPV conductivities, are close to the highest conductivities ($\approx 10^5\ (\Omega\ cm)^{-1}$) measured in I_2-doped polyacetylene.[27] If these normalized conductivities were indeed representative of an *intrinsic* PPV chain conductivity, then the value should be invariant to doping time. As can be seen from Table II the normalized conductivity value fluctuates about $4.4 \times 10^4\ (\Omega\ cm)^{-1}$ for all doping times. Even this calculation underestimates the intrinsic conductivity since at early stages of doping the surface is not fully doped and at later stages the precursor front, which is also not a fully doped region, is included. On the basis of these results a lower limit to the intrinsic conductivity of $4 \times 10^4\ (\Omega\ cm)^{-1}$ is suggested.

Conclusions

The AsF_5-doping of PPV has been shown to result in shallow dopant penetrations when performed with the dopant source of $T < -53$ °C. A dopant penetration of less than 1 μm is achieved for 10-day dopings. The doping process is complicated by the formation of arsenic oxides, which exist as surface layers in the doped films. Further,

the dopant concentration profile is not characteristic of Fickian or case II diffusion. Rather, it is characteristic of simultaneous diffusion and rapid chemical reaction of AsF_5. In PPV doped for 5–10 days a region of nearly constant As concentration is observed just below the surface oxide layer. The relative amounts of arsenic and carbon suggest one dopant anion for every four to five PPV repeat units. When the measured doped layer thicknesses are used, the lower limit to the intrinsic electrical conductivity of AsF_5-doped PPV is estimated to be $\approx 4 \times 10^4$ $(\Omega\ cm)^{-1}$.

Acknowledgment. M.A.M. acknowledges supplemental fellowship support from the Plastics Institute of America. R.J.C. acknowledges support from the NSF/DMR Polymers Program. The use of the facilities of the Cornell Material Science Center made these experiments possible. We thank Nicholas Szabos for technical assistance. Also, we thank Professor R. S. Stein for his support. This work was supported by AFOSR Grant 88-011.

References and Notes

(1) Pekker, S.; Janossy, A. *Handbook of Conducting Polymers*; Skotheim, T. A., Ed.; Marcel Dekker: New York, 1986; p 45.
(2) Chien, J. C. W. *Polyacetylene: Chemistry, Physics, and Materials Science*; Academic Press: New York, 1984;f p 325.
(3) Dresselhaus, M. S.; Wasserman, B.; Wnek, G. E. *Mater. Res. Soc. Symp. Proc.* **1984**, *27*, 413.
(4) Crank, J.; Park, G. S. *Trans. Faraday Soc.* **1951**, *82*, 1072.
(5) Long, F. A.; Richmond, D. *J. Am. Chem. Soc.* **1960**, *82*, 513.
(6) Thomas, N. L.; Windle, A. H. *Polymer* **1977**, *18*, 1195.
(7) Mills, P. J.; Palmstrom, C. J.; Kramer, E. J. *J. Mater. Sci.* **1986**, *21*, 1479.
(8) Kanicki, J. *Handbook of Conducting Polymers*; Skotheim, T. A., Ed.; Marcel Dekker: New York, 1986; p 543.
(9) Burroughes, J. H.; Jones, C. A.; Friend, R. H. *Nature* **1988**, *335*, 137.
(10) Meijer, E. W.; Nijhuis, S.; van Vroonhoven, F. C. B. M. *J. Am. Chem. Soc.* **1988**, *110*, 7209.
(11) Foot, P. J. S.; Mohammed, F.; Calvert, P. D.; Billingham, N. C. *J. Phys. D: Appl. Phys.* **1987**, *20*, 1354.
(12) Benoit, C.; Rolland, M.; Aldissi, M.; Rossi, A.; Cadene, M.; Bernier, P. *Phys. Status Solidi A* **1981**, *68*, 209.
(13) Gagnon, D. R.; Capistran, J. D.; Karasz, F. E.; Lenz, R. W.; Antoun, S. *Polymer* **1987**, *28*, 567.
(14) Bradley, D. D. C.; Friend, R. H.; Lindenberger, H.; Roth, S. *Polymer* **1986**, *27*, 1709.
(15) Masse, M. A.; Martin, D. C.; Petermann, J. H.; Thomas, E. L.; Karasz, F. E. *J. Mater. Sci.* **1990**, *25*, 311.
(16) Masse, M. A.; Schlenoff, J. B.; Karasz, F. E.; Thomas, E. L. *J. Polym. Sci., Polym. Phys.* **1989**, *27*, 2045.
(17) Lenz, R. W.; Han, C. C.; Stenger-Smith, J.; Karasz, F. E. *J. Polym. Sci., Polym. Chem.* **1988**, *26*, 3241.
(18) Machado, J. M.; Karasz, F. E.; Kovar, R. F.; Burnett, J. M.; Druy, M. A. *New Polym. Mater.* **1989**, *1*, 189.
(19) Bradley, D. D. C.; Evans, G. P.; Friend, R. H. *Synth. Met.* **1987**, *17*, 651.
(20) Masse, M. A.; Hirsch, J. A.; White, V. A.; Karasz, F. E. *New Polym. Mater.*, in press.
(21) Chu, W.-K.; Mayer, J. W.; Nicolet, M.-A. *Backscattering Spectrometry*; Academic Press: New York, 1978.
(22) Doolittle, L. R. *Nucl. Instrum. Methods Phys. Res.* **1985**, *B9*, 344.
(23) Masse, M. A. Ph.D. Dissertation, University of Massachusetts, 1989.
(24) Crank, J. *The Mathematics of Diffusion*, 2nd ed.; Oxford University Press: Oxford, 1975.
(25) Obrzut, J.; Karasz, F. E. *J. Chem. Phys.* **1987**, *87*, 6178.
(26) Frommer, J. E.; Elsenbaumer, R. L.; Eckhardt, H.; Chance, R. R. *J. Polym. Sci., Polym. Lett.* **1983**, *21*, 39.
(27) Basescu, N.; Liu, Z.-X.; Moses, D.; Heeger, A. J.; Naarmann, H.; Theophilou, N. *Nature* **1987**, *327*, 403.

Determination of the Fold Surface Free Energy and the Equilibrium Melting Temperature for α-Phase Poly(pivalolactone) Crystals

Hervé Marand*,† and John D. Hoffman*

Michigan Molecular Institute, 1910 West St. Andrews Road, Midland, Michigan 48640

Received October 23, 1989; Revised Manuscript Received February 6, 1990

ABSTRACT: Small-angle X-ray scattering and differential scanning calorimetry were used to determine the long spacings and melting temperature of poly(pivalolactone) samples crystallized isothermally from the melt at growth temperatures in the range 190–210 °C, which spans regimes II and III. Low-angle X-ray spacings and degree of crystallinity data obtained by differential scanning calorimetry were combined to yield accurate values of l, the true crystal core thickness (i.e., the crystal stem length). The use of various heating rates to measure the observed melting temperature allowed the effect of thickening processes to be minimized. Melting temperature and lamellar thickness data were analyzed with the Gibbs–Thomson–Tammann equation to yield the equilibrium melting temperature, $T_m^\circ = 269 \pm 2$ °C, and the fold surface free energy, $\sigma_e = 61 \pm 5$ erg·cm^{-2}.

I. Introduction

Our objective is to provide a careful determination of the equilibrium melting temperature, T_m°, and the fold surface free energy, σ_e, for α-phase poly(pivalolactone) crystals as formed from the subcooled melt. Specifically, we will pay a great deal of attention to the effects of thickening on both the melting point determination and the evaluation of σ_e. The results of such an analysis can then be combined with spherulitic growth rate data to provide an accurate determination of the lateral surface

† Present address: Virginia Polytechnic Institute and State University, Chemistry Department, Blacksburg, VA 24061.

0024-9297/90/2223-3682$02.50/0